DERIVING ALBEDO FOR HAPEX-SAHEL FROM ASAS DATA USING KERNEL-DRIVEN BRDF MODELS

P. Lewis (1), M. I. Disney (1), M. J. Barnsley (2) and J.-P. Muller (3)

[1] Remote Sensing Unit,
Department. of Geography.,
University College London,
26 Bedford Way,
London WC1H 0AP, U.K.

[2] Department. of Geography,
University of Wales, Swansea,
Singleton Park,
Swansea SA2 8PP, U.K.

[3] Department. of Photogrammetry and Surveying,
University College London,
Gower Street,
London WC1E 6BT, U.K.

Paper submitted for publication in: **Hydrology and Earth System Sciences**

Submitted: *18 July 1997*; **Accepted**: __________ *1997*

Abstract

Although it is not an intrinsic surface property, an approximation to albedo can be derived from sparse samples of directional reflectance (remote sensing) data using models of the Bidirectional Reflectance Distribution Function (BRDF). A suite of linear kernel-driven BRDF models have been inverted against airborne directional reflectance data of an area in Niger, West Africa, to produce BRDF model parameters, and from these, integrated reflectance properties related to spectral albedo. Broadband albedo has been estimated from this by weighting the spectral albedos as a function of the appropriate spectral solar irradiance and proportion of direct and diffuse illumination. The derived broadband albedo values appear to agree extremely well with ground-based (point sample) measurements, indicating that this general approach is both sound and practical. The results are, however, shown to be dependent on obtaining the correct spectral weightings. A method for extrapolating albedo data collected over the limited spatial extent of the airborne scanner images is also presented and is used to produce an 'albedo map' over a much larger area.

1. INTRODUCTION

Earth surface albedo is an important parameter in energy budget studies at a wide range of spatial scales. Remote sensing offers the only reliable, accurate and spatially- and temporally-comprehensive way to estimate this quantity on a global scale. Given appropriate atmospheric modelling tools and parameters, optical remote sensing instruments can measure the surface reflectance in a particular direction for given illumination conditions. An estimation of albedo from such data involves integration of the bidirectional reflectance in both the angular and spectral domains. If an accurate estimate is required, a sufficient number of well-placed samples is required in each of these domains along with appropriate models to perform interpolation and extrapolation of the observed reflectance field.

In many senses, the estimation of albedo from such data is one of the more straightforward tasks that can be performed with optical remote sensing data, as the instruments sample a quantity (radiance, thence directional reflectance) which is directly related to the required property. Wanner et al. (1997) describe an algorithm to perform this task, to be used with NASA's forthcoming Earth Observing System (EOS) Moderate Resolution Imaging Spectrometer (MODIS) (Running et al., 1994) and Multiangle Imaging SpectroRadiometer (MISR) (Diner et al., 1989, 1991) instruments. Application of the algorithm involves inverting (linear) kernel-driven models (Wanner et al., 1995) of the surface spectral Bidirectional Reflectance Distribution Function (BRDF) against a sample set of remotely-sensed observations to derive a set of (spectral) model parameters. The models are derived from abstractions of physically-based radiation scattering theory and involve a number of simplifications so that linear kernels can be formed, each representing an element of the abstracted scattering process. The resulting model parameters can be used to derive spectral bihemispherical ($\bar{\bar{\rho}}(\lambda)$) and directional-hemispherical reflectance ($\bar{\rho}(\lambda,\vartheta_s)$ data where ϑ_s is the solar zenith angle and λ refers to wavelength) through angular integration of the kernels; these data can subsequently be used to generate estimates of broadband albedo through spectral integration.

This paper examines the application of this approach to deriving estimates of albedo from directional reflectance data obtained by NASA's airborne Advanced Solid-state Array Spectrometer (ASAS) (Irons et al. 1991). These data were collected over a range of cover types in Niger, West Africa as part of the HAPEX-Sahel field campaign in September 1992 (Prince et al., 1995; Goutorbe et al., 1997). The multi-angle data for each of five sites were coregistered and atmospherically-corrected as described by Barnsley et al. (1997b). After de Colstoun et al. (1996), a continental aerosol model was assumed in performing the atmospheric correction, but the resultant reflectance data tends to be rather sensitive to the aerosol model selected. In order to gain some confidence in the magnitude of the reflectance values derived using this procedure, airborne data over a millet canopy are compared with reflectance data simulated by a detailed 3D canopy reflectance model, the Botanical Plant Modelling System (BPMS) (Lewis, 1996, Lewis and Boissard, 1997).

The ASAS data provide spatial estimates of directional reflectance over several areas, each about 1.5 km^2, at a spatial resolution of 2-3 m. This provides important information on the local spatial variation of the shortwave radiation regime at this scale. Calculation of the ratio of surface-leaving to incoming shortwave fluxes (albedo) involves an angular integral of this information. The angular sampling provided by ASAS is rather limited (up to nine view angles per flightline) and so a model is required to perform directional interpolation, extrapolation and angular integration to spectral albedo. The utility of the kernel-driven models used here has been demonstrated for a range of vegetation canopies and other surfaces (Wanner et al., 1997). The models have a number of attractive properties for the work described in this paper (Lewis, 1995). In particular: (i) they are well-suited to modelling the reflectance of heterogeneous surfaces; (ii) they can be rapidly inverted (which is important when considering the number of spatial directional reflectance samples for all of the ASAS datasets processed is around 30 x 10^6 per waveband); and (iii) angular integrals of reflectance are rapidly achieved by multiplying the model parameters by angular integrals of the kernels.

Conversion of spectral- to broadband estimates of albedo involves integration over the solar spectrum. This is achieved by approximating the integration as a summation over a sample set of wavebands. Validation of the approach is attempted by comparing albedo derived from the ASAS data and kernel-driven models with hourly point-sample measurements of albedo for different cover types acquired on the ground. Finally, a method of spatial extrapolation is investigated to produce albedo maps over a much larger area by combining the albedo estimates derived from ASAS with Landsat Thematic Mapper (TM) data.

2. ASAS REFLECTANCE DATA

2.1 BRDF From ASAS Data

Directional radiance data were recorded by ASAS over five sites in the HAPEX-Sahel area:

1) *East Central Super Site* - fallow (hereafter referred to as ECSS_20);

2*) Southern Super Site* - tiger bush (hereafter referred to as SSS_10);

3) *Southern Super Site* - millet (hereafter referred to as SSS_30);

4) *West Central Super Site* fallow/millet (hereafter referred to as WCSS_10);

5) *West Central Super Site* tiger bush (hereafter referred to as WCSS_30)

These have been processed to produce at-ground directional reflectance (Barnsley et al., 1997b). ASAS obtains imagea at 9 separate view zenith angles (-55° aft to 70° forward). Several flight lines were flown over each site, at a variety of view azimuth and solar zenith angles (Barnsley et al., 1997b, p. 754). Although 62 wavebands are recorded by ASAS (420-1037 nm), only four of these have been processed so far (495, 555, 646 and 862 nm) and are used in this study. The spatial resolution of these data is 2-3 m. The area covered is approximately 1.5 x 1 km in each image.

2.2. COMPARISON OF ASAS REFLECTANCES WITH BPMS-MODELLED DATA

In attempting to derive broadband albedo from spectral directional reflectance data using BRDF model parameters, the accuracy of the resultant albedo will be directly dependent on the quality of the source ASAS reflectance data. A number of factors such as the atmospheric correction process and lack of precision in the accuracy of sensor pointing cause uncertainties in both absolute reflectance values and the associated angular information (viewing and illumination zenith and azimuth angles). Consequently, it is desirable to have some point of comparison - ideally with measured ground reflectance data - to give some confidence in the ASAS reflectance data before model inversion is performed. In the absence of suitable ground-level reflectance data, the comparison made in this study is with at-ground reflectance data generated using a complex 3D canopy reflectance model, the Botanical Plant Modelling System (BPMS) (Lewis, 1996; Lewis and Boissard, 1997).

The BPMS is a model designed to accept plant and terrain geometric data from a wide a variety of sources (including stereo photogrammetric data, direct manual measurements of leaf position, length etc.) and to construct 3D representations of plants in terms of simple model primitives (triangular facets, spheres, cylinders etc.) (Lewis and Boissard, 1997). A ‘field’ of such plants can be constructed according to some measured or simulated planting pattern and planting density. The defined (measured) plant models are distributed over the field (‘cloned’) according to some probability of occurrence for each plant model. All of the elements within the scene are assigned material properties, describing, for instance, leaf optical properties. Accurate radiometric simulations of the canopy can then be carried out using Monte Carlo ray tracing (MCRT) (Lewis and Muller, 1992). A major advantage of the BPMS is the potential it provides to derive detailed information on the radiation regime of complex plant canopies (e.g., contributions to reflectance as a function of scattering order, proportions of sunlit and shaded scene components, contributions from direct and diffuse illumination, detailed characterisation of leaf angle distribution and leaf area density etc.).

Detailed manual geometric measurements were made of five millet plants in the HAPEX-Sahel Southern Super Site millet area (SSS_10) during September 1992. These data are used within the BPMS to construct 3D models of the millet plants (Figure 1). The millet canopy is constructed by randomly distributing ‘clones’ of the five measured plants on a rectangular grid with a row and plant spacing of 2m (determined from field measurements). The PROSPECT leaf scattering model (Jacquemoud and Baret 1990) is used to generate leaf and stem spectral reflectance and transmittance information in the absence of appropriate measured leaf spectral data. Soil spectral directional reflectance data (van Leeuwen and Huete, 1997) measured *in situ* in the Sahel are used to represent soil reflectance in the model. MCRT simulations were carried out over a range of view zenith angles using an isotropic sky radiance function, at each of the four ASAS wavebands used (495, 555, 646 and 862 nm), and with the same illumination conditions those under which the ASAS data were acquired to give a complete simulated directional reflectance data set.

Comparisons between the simulations and millet reflectances extracted from a relevant area within the ASAS data are shown in Figure 2. A Lambertian soil reflectance (mean of the measured directional soil reflectance data) is assumed for simulations presented in figure 2(a), and measured directional soil reflectance data were used in the results of figure 2(b), to examine the impact of assuming a Lambertian soil. The absolute values of the ASAS and BPMS reflectances in figure 2 are sufficiently similar to give confidence in the preprocessing of the ASAS data (after atmospheric correction). The shapes of the respective BRDFs are, however, slightly different, the BPMS simulations being noticeably flatter. Lewis and Disney (1997) demonstrate that the majority of directional ('shape') information is controlled by the proportion of sunlit soil contributing to the canopy reflectance using an analysis of the same BPMS data. One potential conclusion from this then, is that the canopy used in the BPMS simulation does not correctly model the proportion of sunlit soil viewed, perhaps because of irregularities (e.g., paths through the canopy) in the 'real' canopy structure viewed by the ASAS data. An alternative explanation could be that the atmospheric correction applied to the ASAS data underestimates the atmospheric path radiance, resulting in a more pronounced reflectance anisotropy in the ASAS data. No firm conclusion can be made from this analysis regarding the cause of the differences between measured and modelled reflectance. At this point, it is sufficient to note that the BPMS simulations provide some evidence that the absolute values obtained from the atmospherically-corrected ASAS data are broadly correct.

3. ESTIMATION OF SPECTRAL ALBEDO FROM ASAS REFLECTANCE DATA

3.1 Kernel-Driven BRDF Models

A kernel-driven model (Roujean et al., 1992) defines the spectral bidirectional reflectance factor, $\rho(\lambda,\ \vartheta_v,\ \vartheta_v,\ \varphi)$ - a function of wavelength λ, view zenith angle ϑ_v, solar zenith angle ϑ_s, and relative azimuth angle φ - as:

$$\rho(\lambda,\ \vartheta_v,\ \vartheta_s,\ \varphi) = f_{iso}(\lambda) + f_{vol}(\lambda)\ k_{vol}(\vartheta_v,\ \vartheta_s,\ \varphi) + f_{geo}(\lambda)\ k_{geo}(\vartheta_v,\ \vartheta_s,\ \varphi) \qquad (1)$$

where: f_{iso} is the Isotropic parameter (a normalisation term representing the reflectance at nadir with a solar zenith angle of zero); f_{vol} is the volumetric scattering parameter (based on an approximation to single-scattering from a homogeneous volume-scattering medium after Ross (1981)); f_{geo} is the geometric parameter (based on considerations of sunlit and shaded canopy proportions from discrete objects after Li and Strahler (1986)); and k_{vol} and k_{geo} are the kernels associated with the latter two terms (Wanner et al., 1995). The kernels are, in effect, 'shapes' describing the abstraction of the BRDF given different sets of assumptions about the major scattering processes and a range of simplifications which permit linearisation. The kernels are not orthogonal in the general case (Wanner et al., 1996) and the accuracy of the resultant model parameters will depend on the angular sampling. Typically, the Isotropic parameter has the lowest degree of uncertainty, although this depends on the average solar zenith angle of the observations. The expected error in the other terms decreases with increasing kernel variance and decreasing covariance over the angular sample set. Various sets of approximations can be made in the linearisation stage of model development, for instance assuming the volumetric component to be optically thin (a kernel known as RossThin) or thick (RossThick). The geometric kernels, known generically as Li kernels involve various approximations and non-linear terms which must be held constant in this process, from which we derive two major kernels, known as LiSparseModis and LiDenseModis (Wanner et al., 1997). The resultant model parameters have no direct physical meaning due to the abstractions involved but Lewis and Disney (1997) suggest that, under some circumstances, aspects of the original physical meaning of the parameters (e.g., a coupled leaf area index-leaf reflectance (LAI) term in the volume-scattering parameter) are maintained.

3.2 BRDF Model Inversions and Calculation of Spectral Albedo

The kernel-driven models are inverted against the ASAS reflectance data. The inversion is constrained to keep the model parameters within physically-valid limits - in effect, imposing non-negativity on the model parameters (Lewis, 1995). The time required for inversion depends on the number of samples and wavebands used, but is of the order of minutes per 1 x 1.5 km scene on a single R10000 processor.

Different kernels (RossThin/RossThick and LiSparseModis/LiDenseModis) are combined to form separate model combinations (along with an Isotropic component). The choice of which set of kernels is best suited to a particular pixel can be made by using a weighted function of the root-mean-squared error in model inversion (Wanner et al., 1997). One problem with a selection procedure of this sort, however, is that a number of different kernel combinations can produce similar goodness-of-fit values. Vives de Lope and Lewis (1997) suggest that examining the consistency of this measure over time can improve the reliability of kernel selection for multitemporal studies, but the data used in this study are for a single time period only. In this case, it is perhaps more appropriate to examine the *spatial* consistency of the error measure in attempting to select the most suitable kernel combination. In addition, one can gain some insight into the appropriateness of kernel combinations by examining the spatial proportion of model parameters that lie on the constraint boundaries - in effect, those that are constrained to zero. An analysis based on these two conditions suggests that the most appropriate kernel combination for these data is (Isotropic and) RossThin (volumetric) LiSparseModis (geometric).

Model parameter information obtained from inversion of these kernels against the reflectance data is shown in figure 3. From top to bottom the images show the Isotropic, RossThin and LiSparseModis parameter information of the red band (646 nm). Figures 3a to e, respectively, show the parameters for each of the five locations noted above.

Figure 3 suggests that the majority of the reflectance information is contained within the Isotropic parameter, and consequently the albedo will largely be controlled by this. The geometric and volume-scattering kernels, the directional components of surface reflectance, contain successively lower magnitude information (and tend to have higher proportionate uncertainties associated with them), but the variation described by these is still significant as the surface reflectance is still distinctly non-Lambertian. This result confirms the findings presented by Barnsley et al. (1997a) who examined the statistical information content of directional reflectance data over an agricultural area in the UK, and concluded that the magnitude of differences in the 'shape' of BRDF over an area can be significantly less than scene 'brightness variations' (analogous to the volume-scattering/geometric and isotropic parameters respectively). The results shown in figure 3 demonstrate the ability of linear BRDF models to extract information on the spatial variability of a parameterisation of directional reflectance, whilst highlighting the difficulty of accurately characterising the directional component (which may be orders of magnitude smaller than the

Isotropic component). It is interesting to note that for the tiger bush sites, the constrained inversion of the RossThin parameter is non-zero only for the vegetation. Similarly, the LiSparseModis parameter is non-zero only for the bare soil areas. This supports the evidence of Lewis and Disney (1997) who analyse the directional reflectance of millet, that the RossThin parameter can indeed model the scattering of vegetation and the LiSparseModis the soil.

Spectral directional-hemispherical reflectance is a function of solar zenith angle. In the kernel-driven modelling approach, this is calculated through:

$$\bar{\rho}(\lambda, \vartheta_s) = f_{iso}(\lambda) + f_{vol}(\lambda) K_{vol}(\vartheta_s) + f_{geo}(\lambda) K_{geo}(\vartheta_s) \quad (2)$$

where K_{vol} and K_{geo} are directional-hemispherical integrals of k_{vol} and k_{geo} respectively (Roujean et al., 1992; Lewis, 1995). The bihemispherical integral of reflectance is similarly calculated using bihemispherical integrals of the kernels. Note from equation 2 that the kernel integrals can be precalculated; the resultant integrated reflectance terms are then simply weighted summations of the model parameters and hence fast to calculate.

Figure 4 shows a comparison of the spectral directional-hemispherical reflectance of the SSS_10 millet canopy as a function of solar zenith angle calculated from the ASAS data and that simulated using the BPMS. The modelling of directional-hemispherical reflectance provided by the BPMS is seen to be relatively close to that produced from the kernel-driven models and ASAS data. The difference between the two tends to decrease with decreasing solar zenith angle which gives us some confidence in the extrapolation trend of this quantity calculated from the kernel-driven models with observations at a range of solar zenith angles of 34 to 46^{o} (Barnsley et al., 1997b).

Correct modelling of spectral directional-hemispherical reflectance is more important for energy budget studies at lower solar zenith angles, due to the higher ground-projected irradiance at these angles. The discrepancy between the two is carried through from the differences in BRDF shape observed in figure 2.

Using the information generated from the model inversions, spectral directional-hemispherical reflectance, $\overline{\rho}(\lambda,\vartheta s)$ (equation 2) and bihemispherical reflectance $\overline{\overline{\rho}}(\lambda)$ are calculated for each waveband. Spectral albedo, $\alpha(\lambda)$, can be estimated from these by:

$$\alpha(\lambda) = \left(1 - d(\lambda,\vartheta_s)\right) \overline{\rho}(\lambda,\vartheta_s) + d(\lambda,\vartheta_s) \overline{\overline{\rho}}(\lambda) \tag{3}$$

where $d(\lambda,\vartheta s)$ is the proportion of diffuse illumination. This approximation involves assuming the sky illumination to be isotropic, which is reasonable in the calculation of albedo, other than at high solar zenith angles (Lewis and Barnsley, 1994).

4. CALCULATION OF BROADBAND ALBEDO FROM SPECTRAL ALBEDO

The calculation of broadband albedo α , from the terms above is given by:

$$\alpha = \int_{solar} W(\lambda, \vartheta s) \left[\overline{\rho}(\lambda,\vartheta s) \left(1 - d(\lambda,\vartheta s)\right) + d(\lambda,\vartheta s) \overline{\overline{\rho}}(\lambda)\right] d\lambda \tag{4}$$

where $W(\lambda,\vartheta s)$ is the proportion of total irradiance at that wavelength and solar angle. The integration is performed over the entire solar spectrum.

More practically, we have some sample set of wavebands over which to obtain an estimate of the integral. If the wavebands sample the solar spectrum sufficiently well, we can approximate the integral in equation 4 by a weighted summation over a finite number of wavebands. This approach is adopted here. Information on the direct and diffuse illumination as a function of time (and hence, solar zenith angle) is calculated using the atmospheric radiation transfer code, 6S (Vermote et al. 1997a) with measured atmospheric parameters. Note from equation 4 that, even if the spectral reflectance (hence spectral albedo) is Lambertian, this is not necessarily so for the broadband albedo as it depends on the varying proportions of *W* as a function of solar zenith angle. This is clearly demonstrated in figure 5, which shows that the proportional contributions may change significantly over the day. For solar zenith angles beyond 70^{o} the information in figure 5 may be unreliable as the 6S simulation is not valid (i.e. before 07:14 and after 16:40). Lewis and Barnsley (1994) also note that an isotropic diffuse approximation in the calculations of albedo is poor at low solar elevations.

Figure 6 shows the broadband albedo calculated for the SSS_10 site from the model-derived integrated reflectance terms. In order to obtain sufficient angular samples, ASAS data from the 3rd and 9th of September were combined. Also shown are measured values of broadband albedo for these dates, giving close agreement with the modelled values, except at extreme solar zenith angles. Modelled spectral albedo values for the site are also shown - the broadband albedo is simply a linear weighting of these terms. The wide range of spectral albedo emphasises the importance of correct estimation of the weighting terms. The over-estimation of albedo at large solar zenith angles may be due to an over-estimation of the near infrared contribution to the spectral weighting at these angles. However, this could equally be attributed to the fact that the assumption of isotropic diffuse irradiance is poor at high solar zenith angles (Lewis and Barnsley, 1994).

Figure 7 shows similar information to figure 6, but for the SSS_30 site. The data are separated into measured and modelled albedo for bare soil and tiger bush shrubs. These data are for a single date (17^{th} September). Again, a close agreement is shown, although the soil albedo derived from ASAS appears tp be a slight over-estimate. This may be because the measured data are 'contaminated' by some vegetation within the sensor's field of view, which will serve to lower the measured albedo values. Figure 8 shows a scatterplot of modelled surface radiance against measured values for all sites. The correlation coefficient 0.979, confirms the close agreement between the measured and modelled data. The only noticeable outliers are the values obtained using the ASAS data of SSS_10 for the 3^{rd} September in isolation. These data contain only 7 angular samples (as opposed to 25 samples for the 9^{th} September and 19 samples for the SSS_30 site (17^{th} September)) which result in larger errors in the modelled albedo values. Figure 8 illustrates that a larger error in estimated albedo is of much less importance at high solar zenith angles, as the solar irradiance at these times of day is so much lower than at either side of solar noon. Figure 9 shows ASAS derived broadband albedo at 12:00 GMT over the five separate sites. The areas of very high albedo are bare soil; the areas of low albedo, dense vegetation, such as tiger bush.

5. SPATIAL EXTRAPOLATION OF ALBEDO USING TM DATA

ASAS data and kernel-driven BRDF models appear to be able to provide reasonable estimates of albedo over the areas imaged by the instrument. These data are useful in their own right for localised energy budget studies, but data over a much wider area are required for smaller scale studies. One approach to achieving this is to use moderate-resolution satellite data from instruments such as NOAA's Advanced Very High Resolution Radiometer (AVHRR) (1.1 km at nadir) (Vives de Lope and Lewis, 1997). Such data have the additional advantage of being able to provide multitemporal estimates of albedo by combining directional reflectance information over some temporal window. The accuracy of any derived albedo product will, like the ASAS results, be critically dependent on the quality atmospheric correction applied. Thus while Vives de Lope and Lewis attempt to make use of AVHRR data to monitor albedo over the HAPEX-Sahel area, they note the large uncertainty introduced by this factor. Global processing of the albedo product using data from NASA's MODIS and MISR sensors will also be dependent on the quality of the atmospheric correction, but a major effort is being put into this area (Vermote et al., 1997b) so the quality of the product should be significantly higher. In addition, the combination of MODIS and MISR data provides better angular sampling than that available using the AVHRR in isolation.They will also have narrower wavebands covering the solar spectrum, and will be better calibrated. Thus, whilst an attempt can be made at providing estimates of albedo from existing sensors such as AVHRR (particularly important for historical studies), the launch of the EOS sensors will see the start of much higher quality data with which to derive this information.

An alternative method to using moderate resolution satellite data is developed here. In this approach, model parameter information generated from the ASAS data are extrapolated through to the scale of Landsat TM (30m). A demonstration of the technique is presented in this paper for the area covering the Southern Super Site of the HAPEX-Sahel area. Within this area, ASAS data are available for regions of millet and tiger bush. The technique relies on three main assumptions, namely that:

(i) the cover types contained within the ASAS images are representative of those in the wider area covered by the TM data;

(

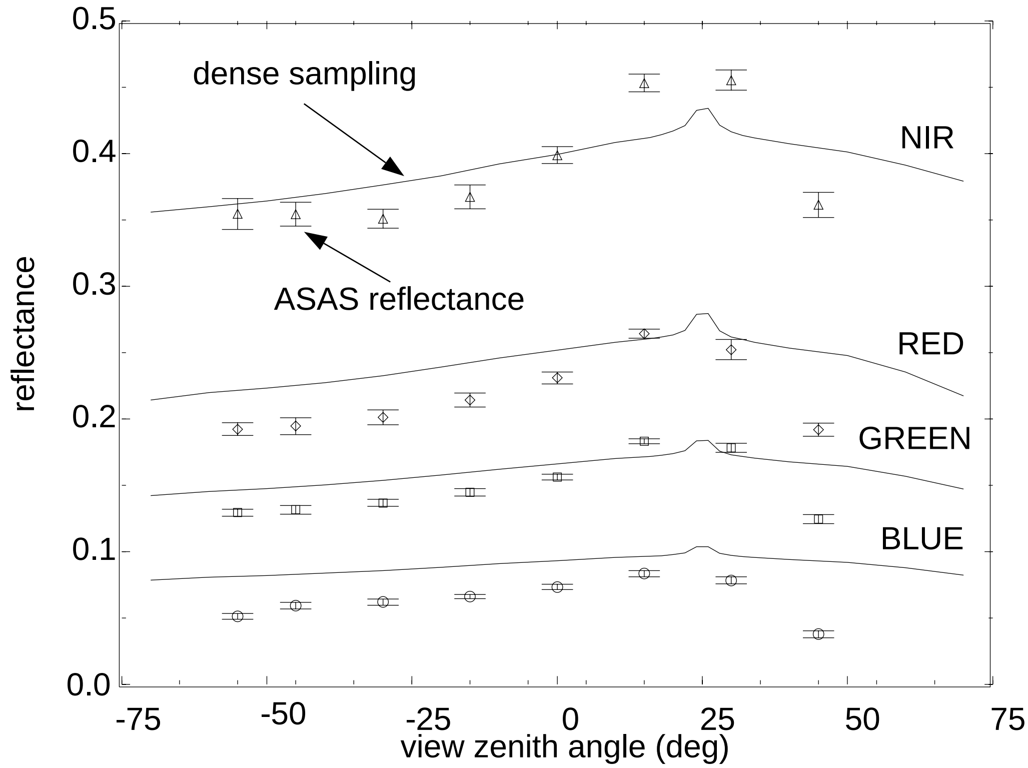

0.5
0.4
0.3
0.2
0.1
0.0
reflectance
dense sampling
ASAS reflectance
NIR
RED
GREEN
BLUE
-75
-50
-25
0
25
50
75
view zenith angle (deg)

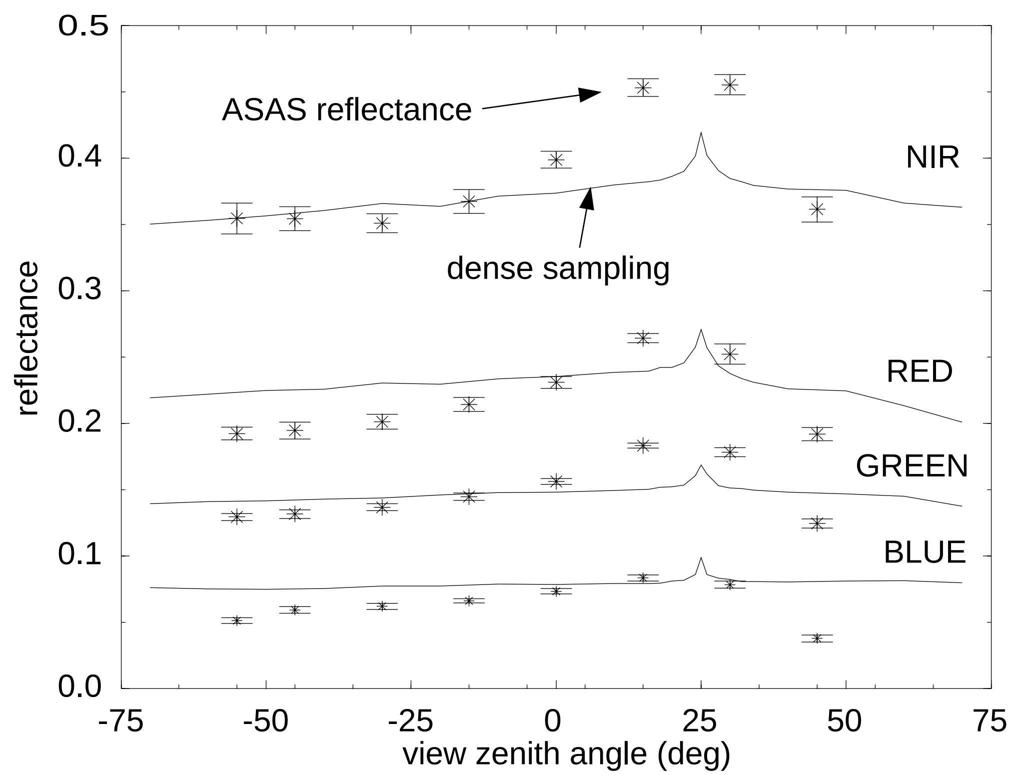

0.5
0.4
0.3
0.2
0.1
0.0
reflectance
ASAS reflectance
dense sampling
NIR
RED
GREEN
BLUE
-75
-50
-25
0
25
50
75
view zenith angle (deg)

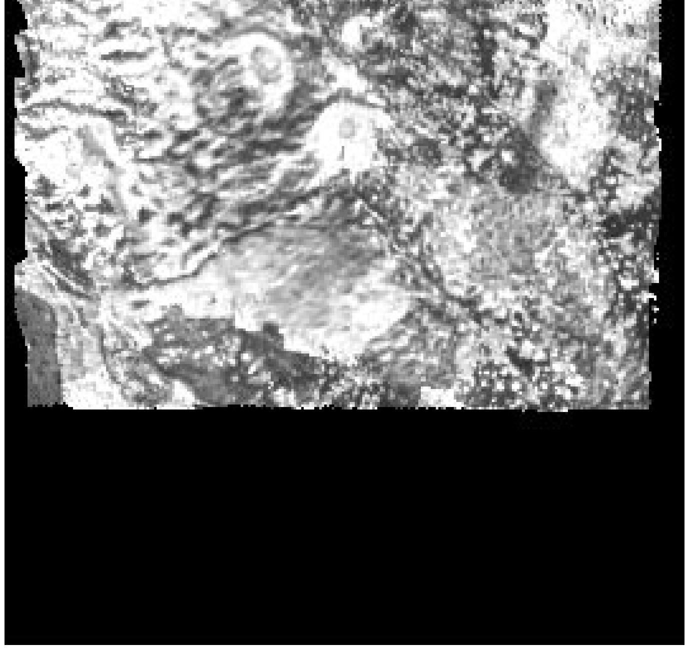

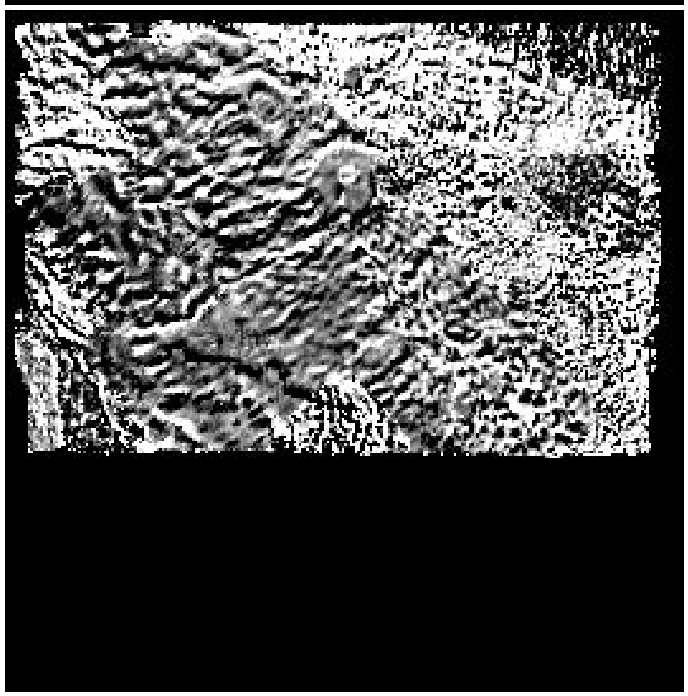

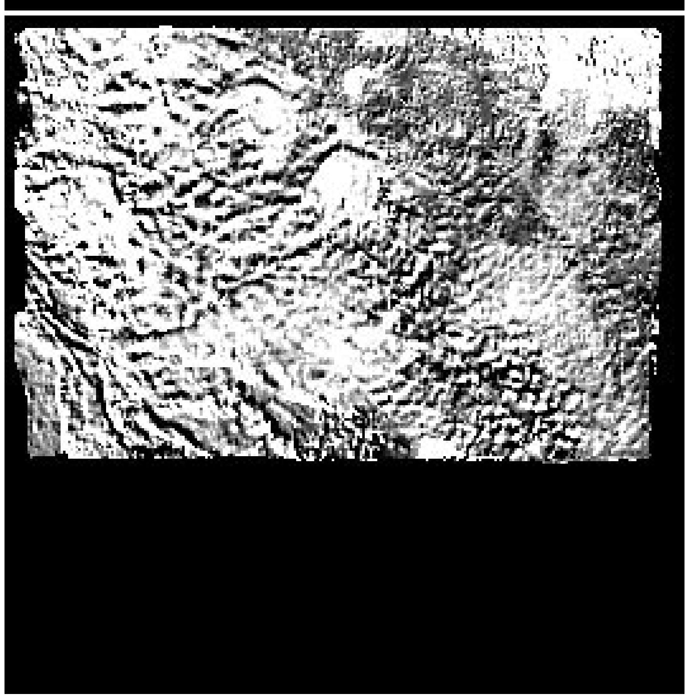

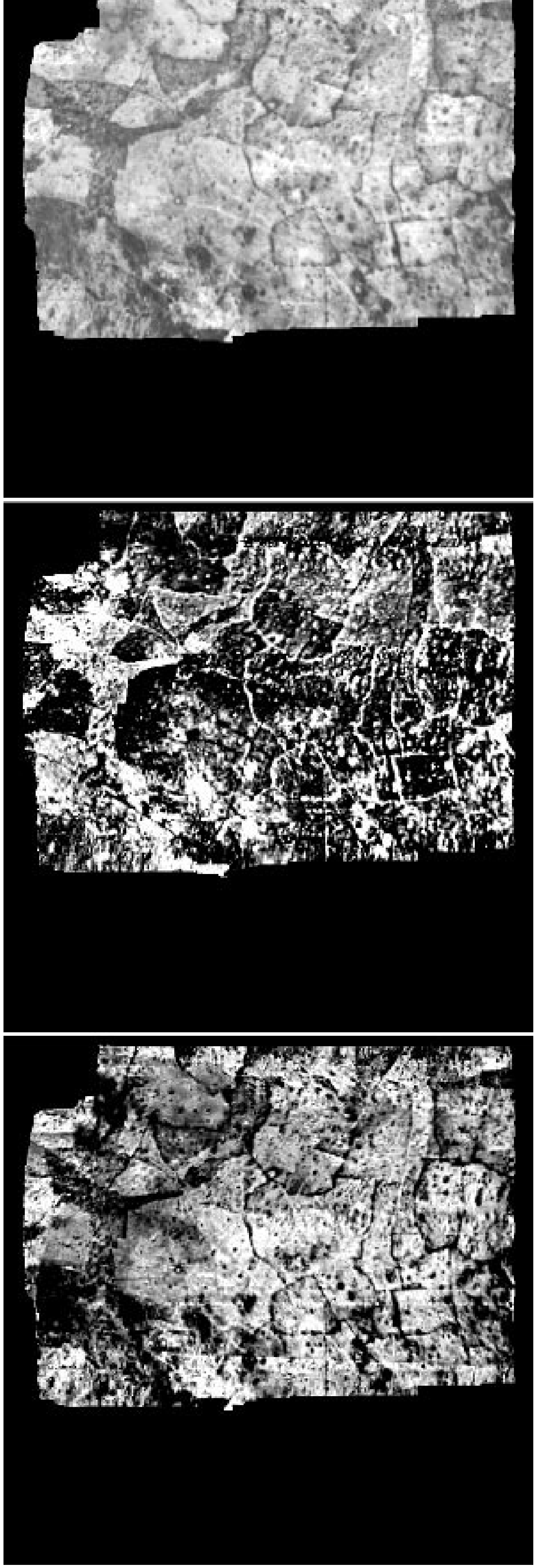

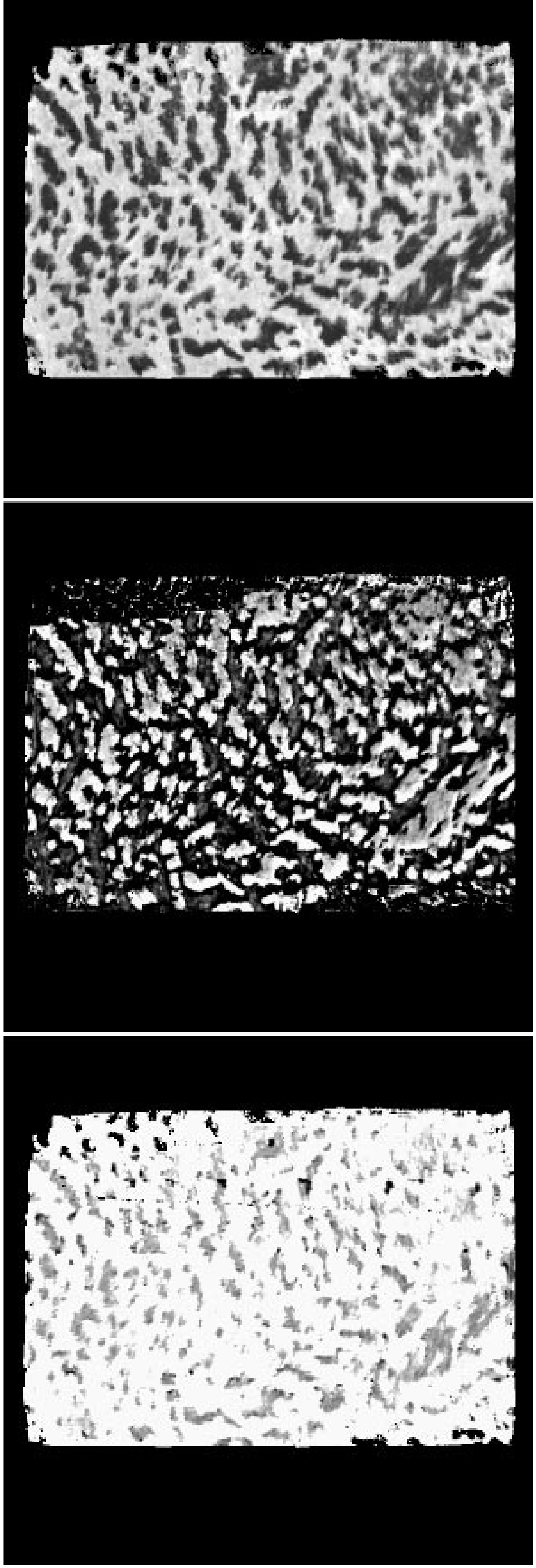

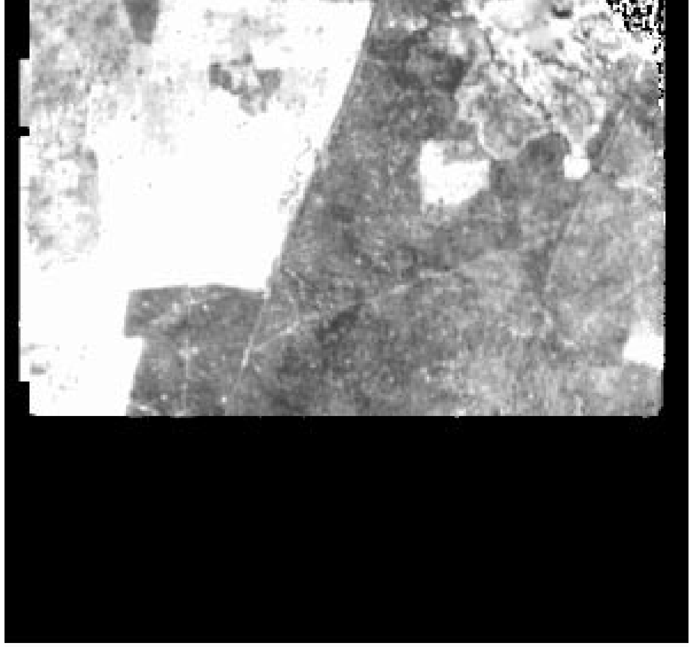

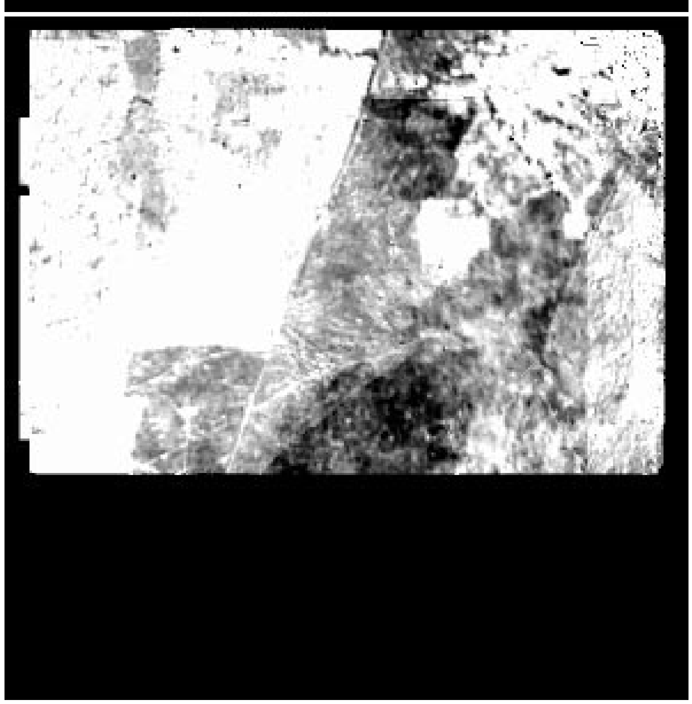

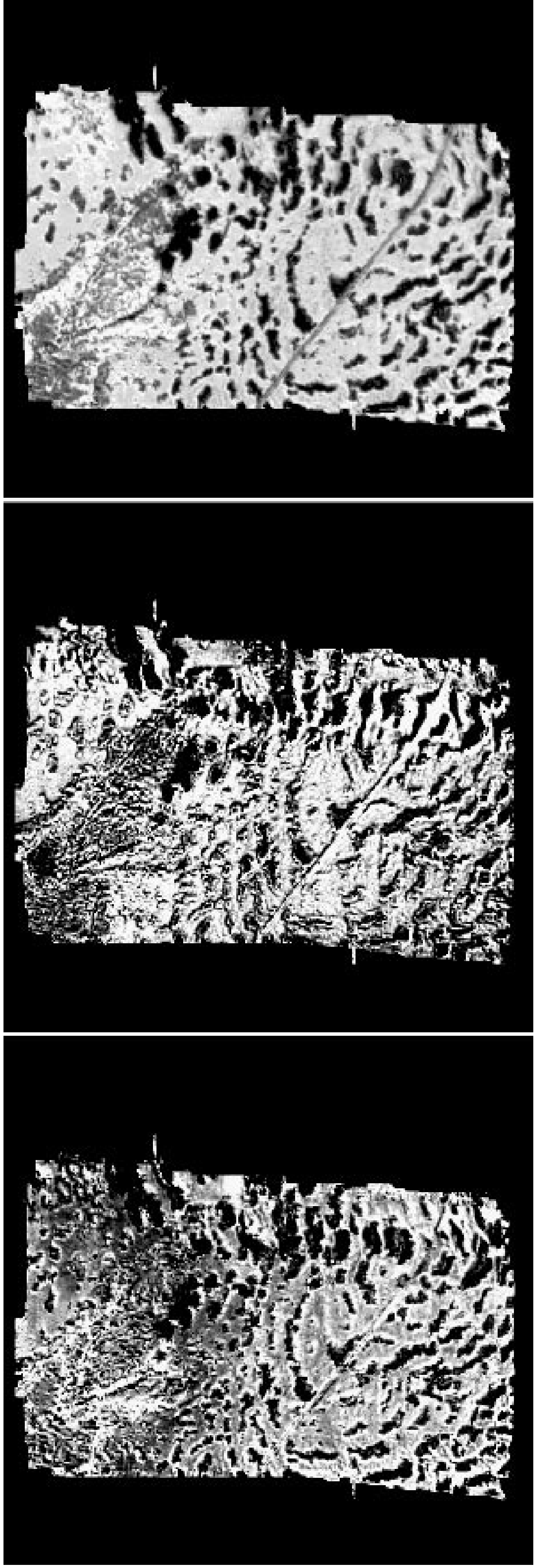

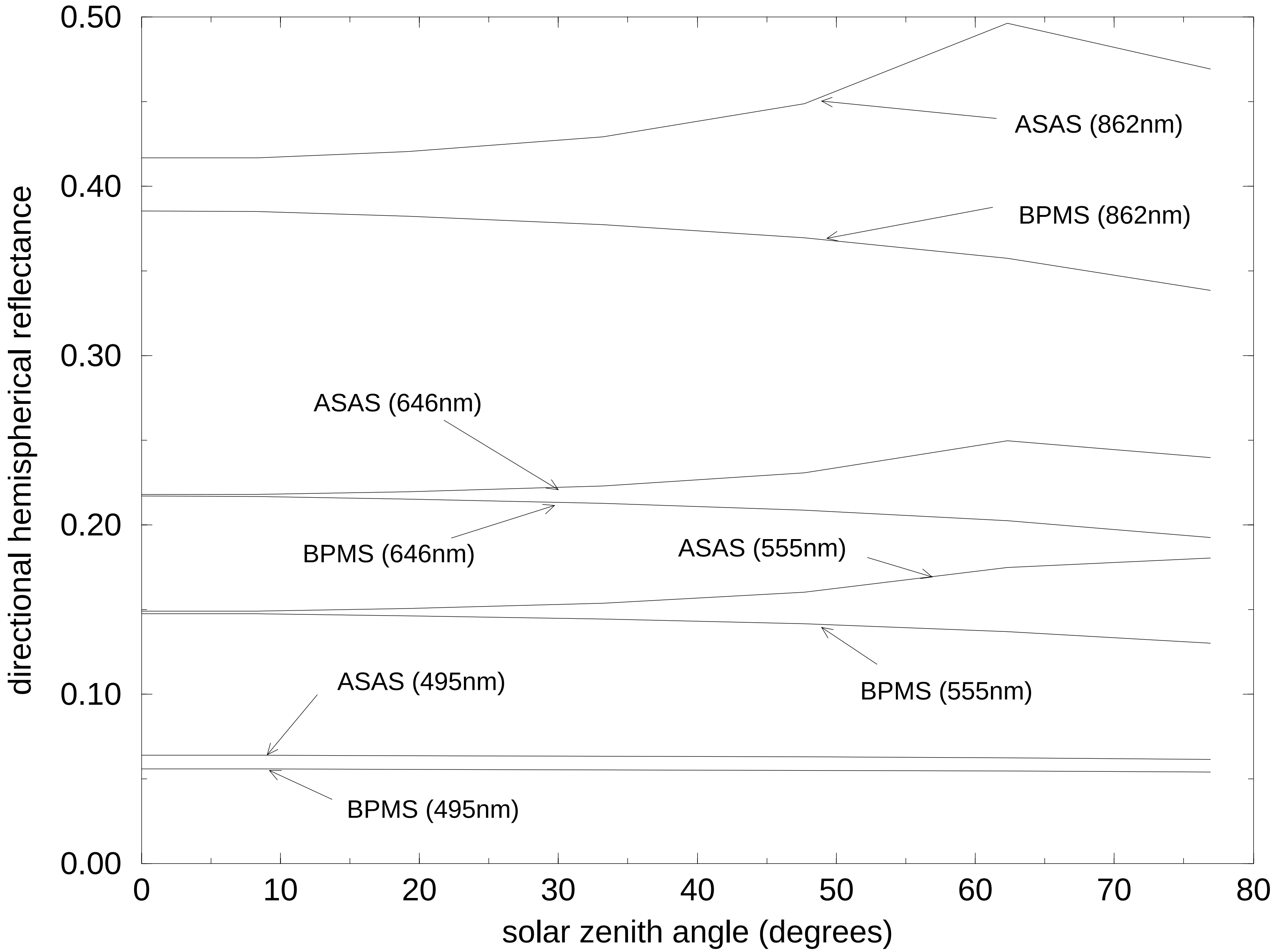

directional hemispherical reflectance
solar zenith angle (degrees)
0.00
0.10
0.20
0.30
0.40
0.50
0
10
20
30
40
50
60
70
80
ASAS (862nm)
BPMS (862nm)
ASAS (646nm)
BPMS (646nm)
ASAS (555nm)
BPMS (555nm)
ASAS (495nm)
BPMS (495nm)

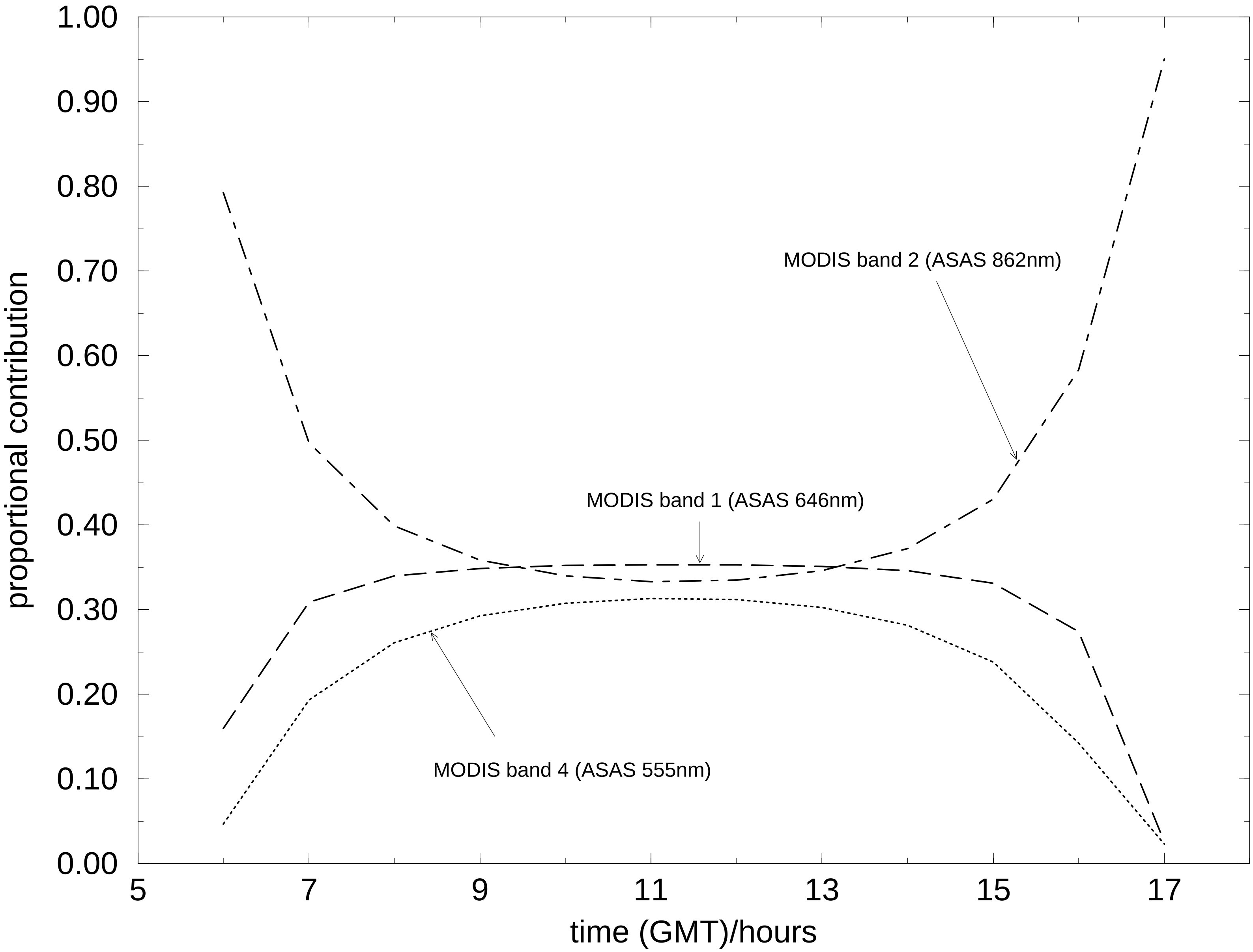

1.00
0.90
0.80
0.70
0.60
0.50
0.40
0.30
0.20
0.10
0.00
proportional contribution
5
7
9
11
13
15
17
time (GMT)/hours
MODIS band 2 (ASAS 862nm)
MODIS band 1 (ASAS 646nm)
MODIS band 4 (ASAS 555nm)

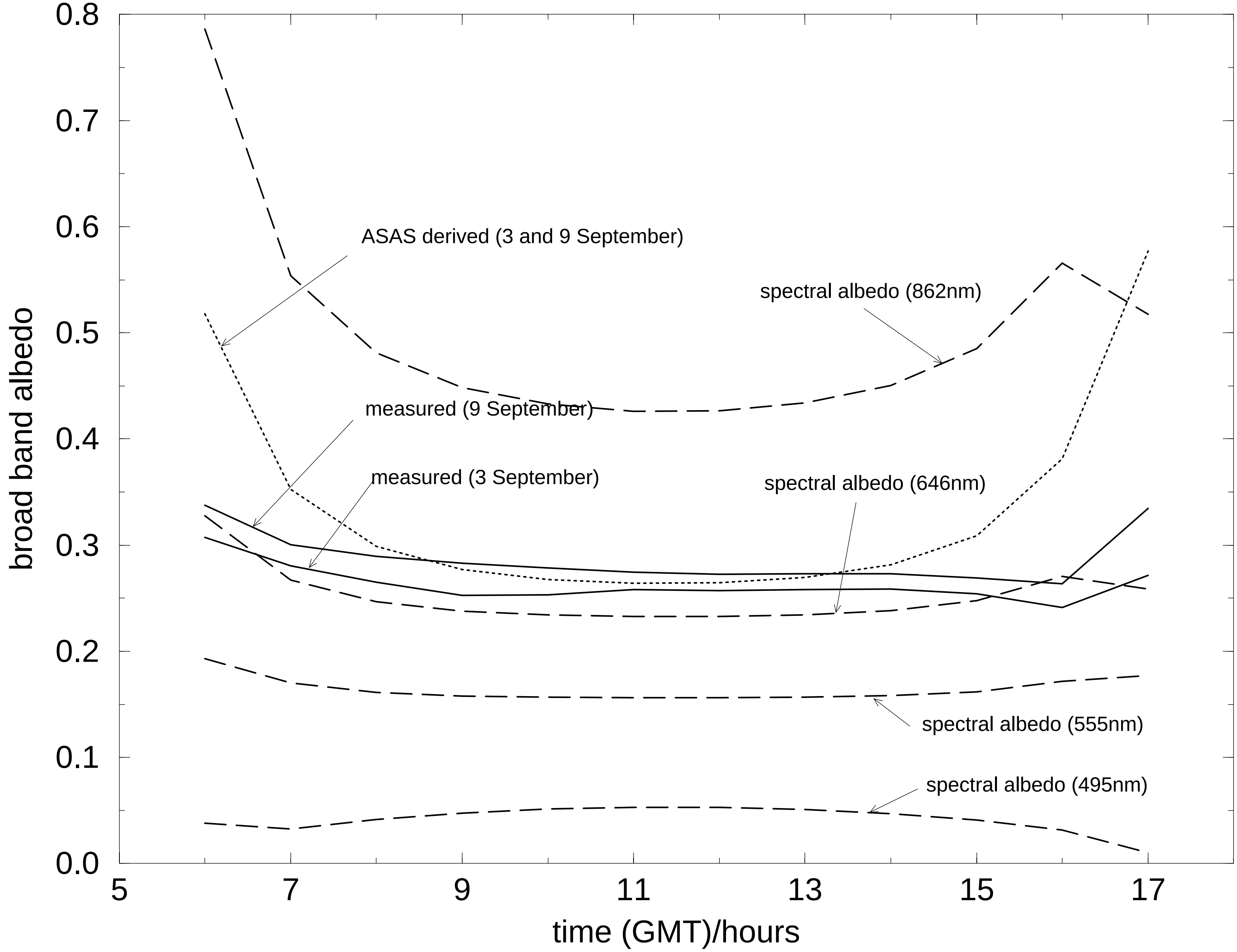

0.8
0.7
0.6
0.5
0.4
0.3
0.2
0.1
0.0
5
7
9
11
13
15
17
broad band albedo
time (GMT)/hours
ASAS derived (3 and 9 September)
spectral albedo (862nm)
measured (9 September)
measured (3 September)
spectral albedo (646nm)
spectral albedo (555nm)
spectral albedo (495nm)

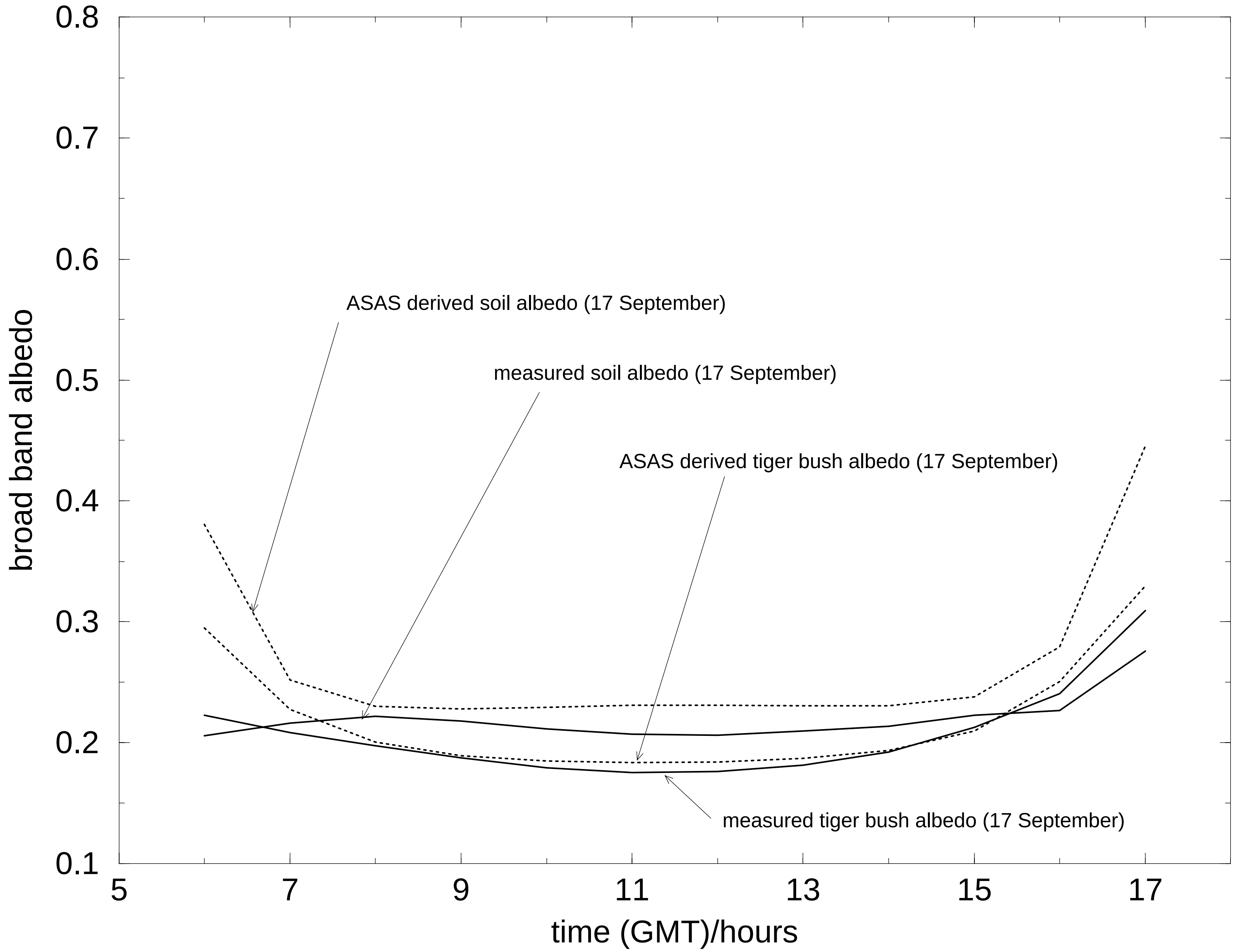

ASAS derived soil albedo (17 September)
measured soil albedo (17 September)
ASAS derived tiger bush albedo (17 September)
measured tiger bush albedo (17 September)
broad band albedo
time (GMT)/hours
0.8
0.7
0.6
0.5
0.4
0.3
0.2
0.1
5
7
9
11
13
15
17

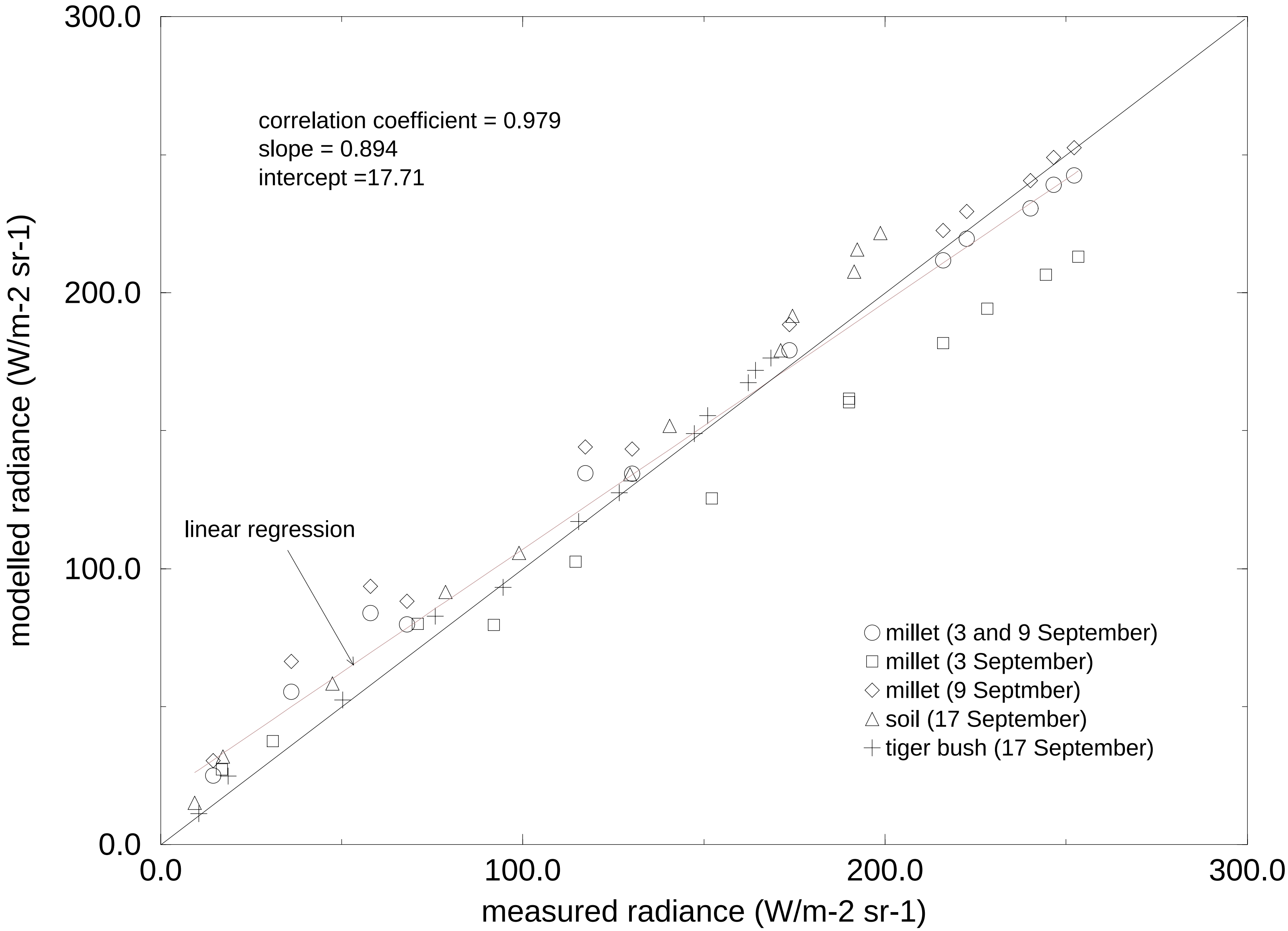

correlation coefficient = 0.979
slope = 0.894
intercept =17.71
linear regression
millet (3 and 9 September)
millet (3 September)
millet (9 Septmber)
soil (17 September)
tiger bush (17 September)
modelled radiance (W/m-2 sr-1)
measured radiance (W/m-2 sr-1)
0.0
100.0
200.0
300.0

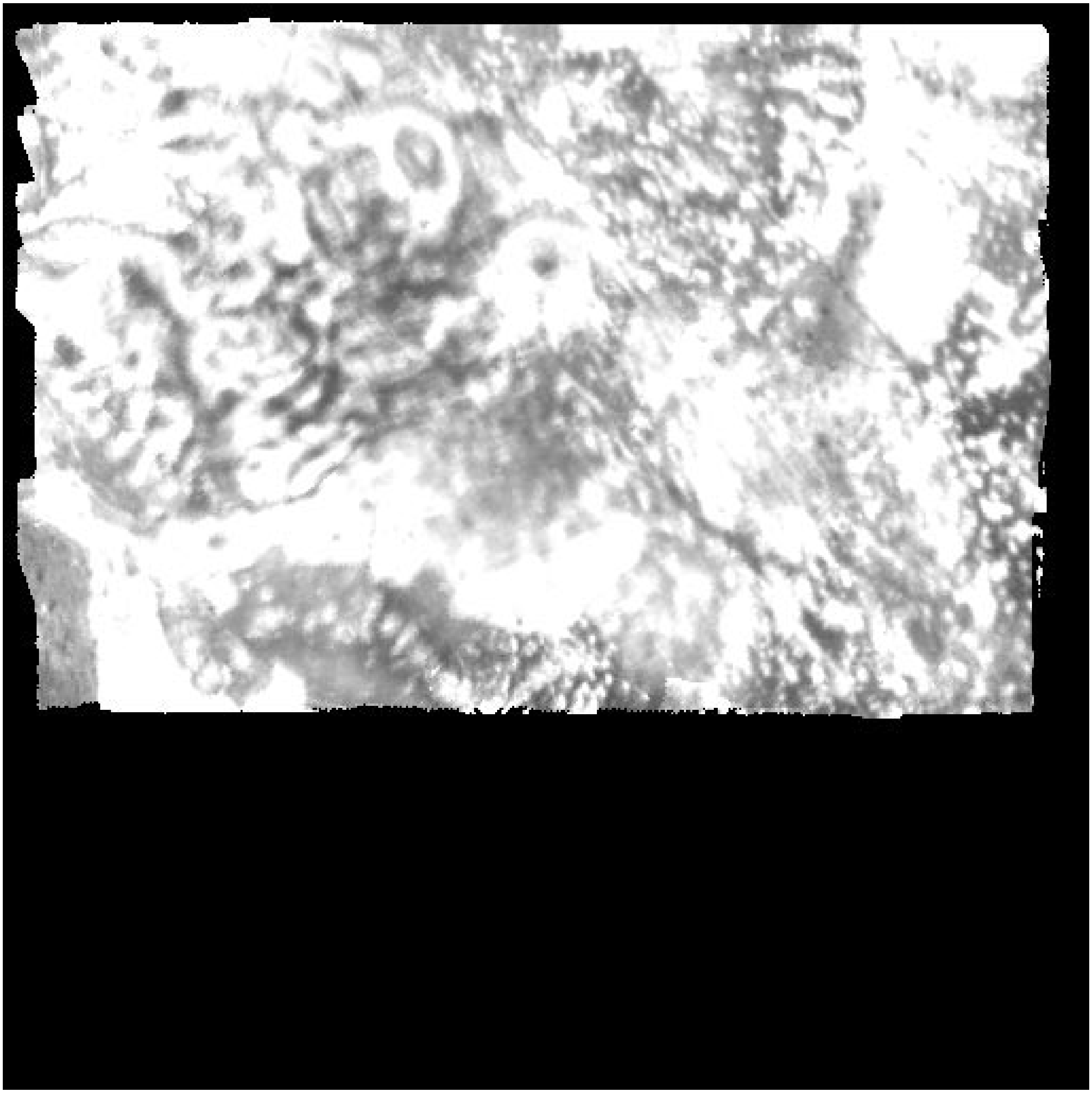

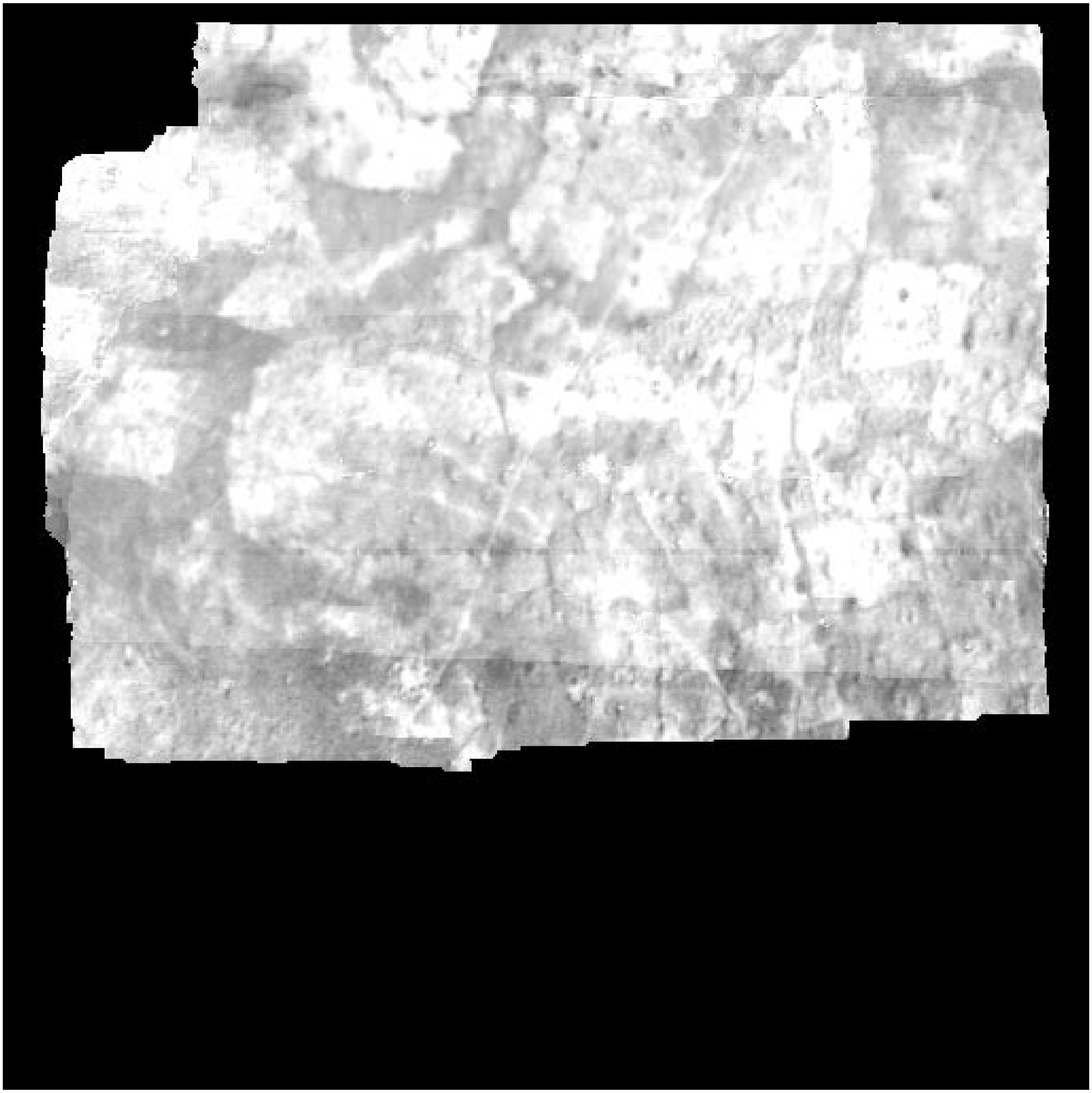

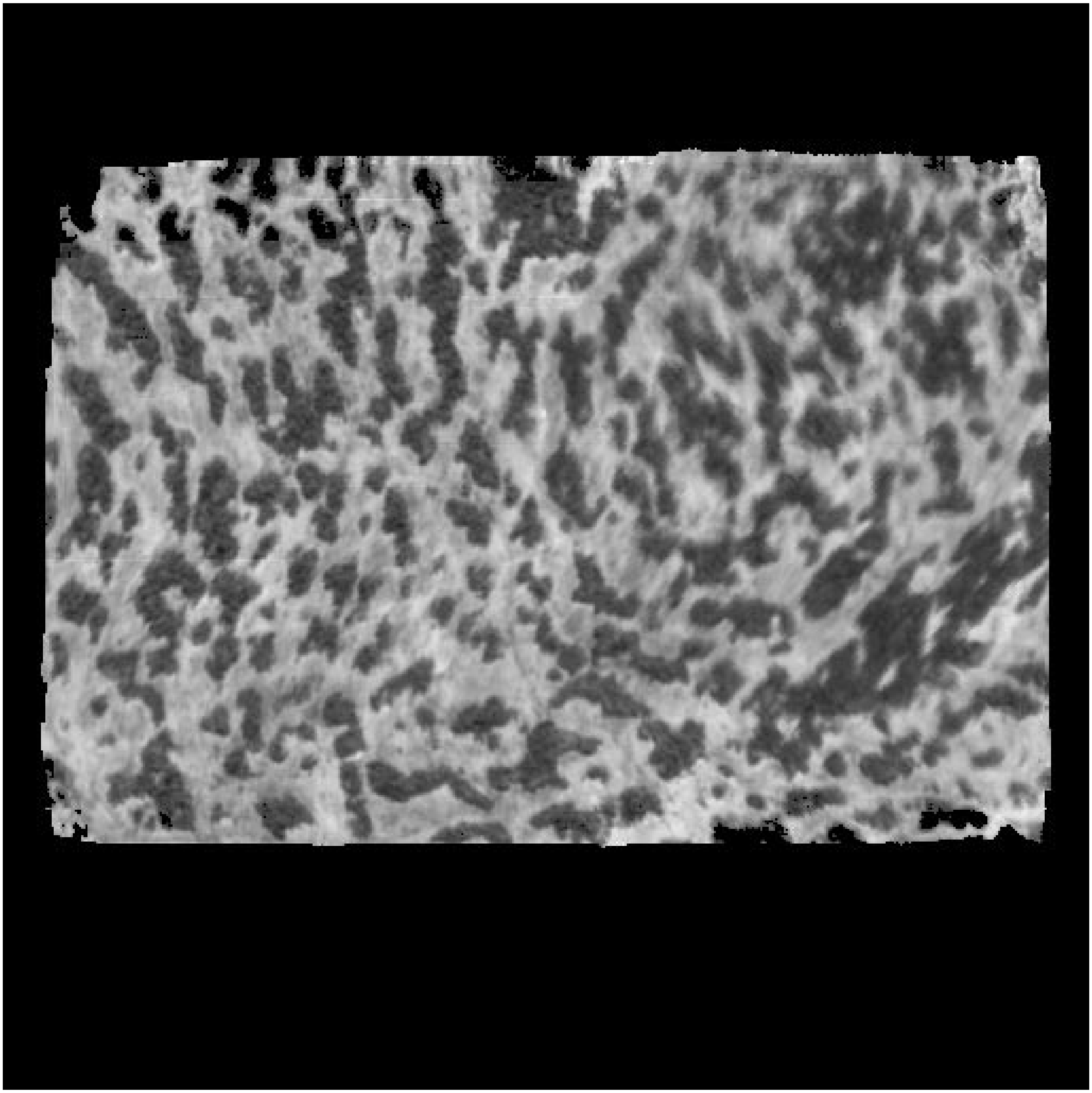

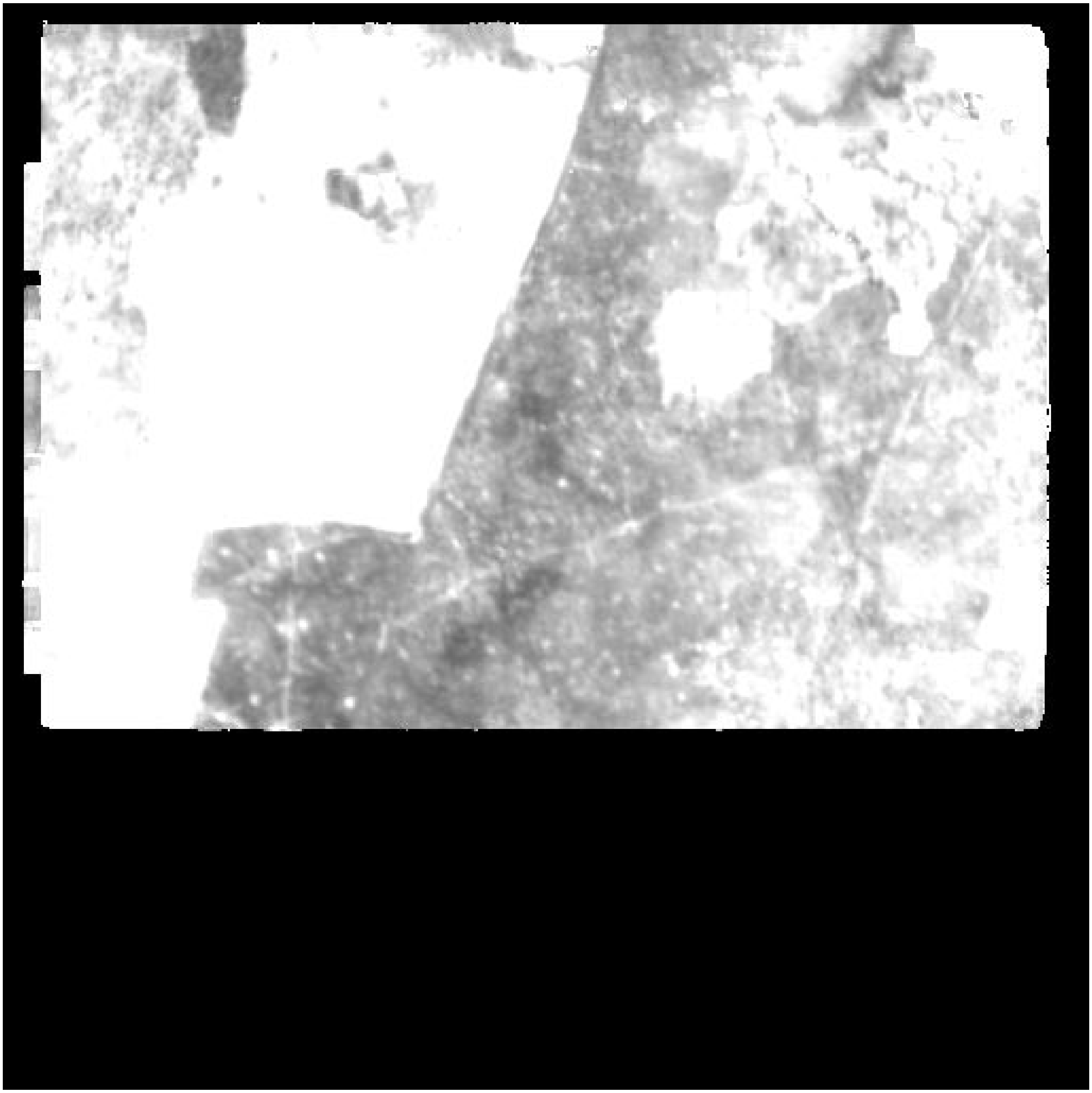

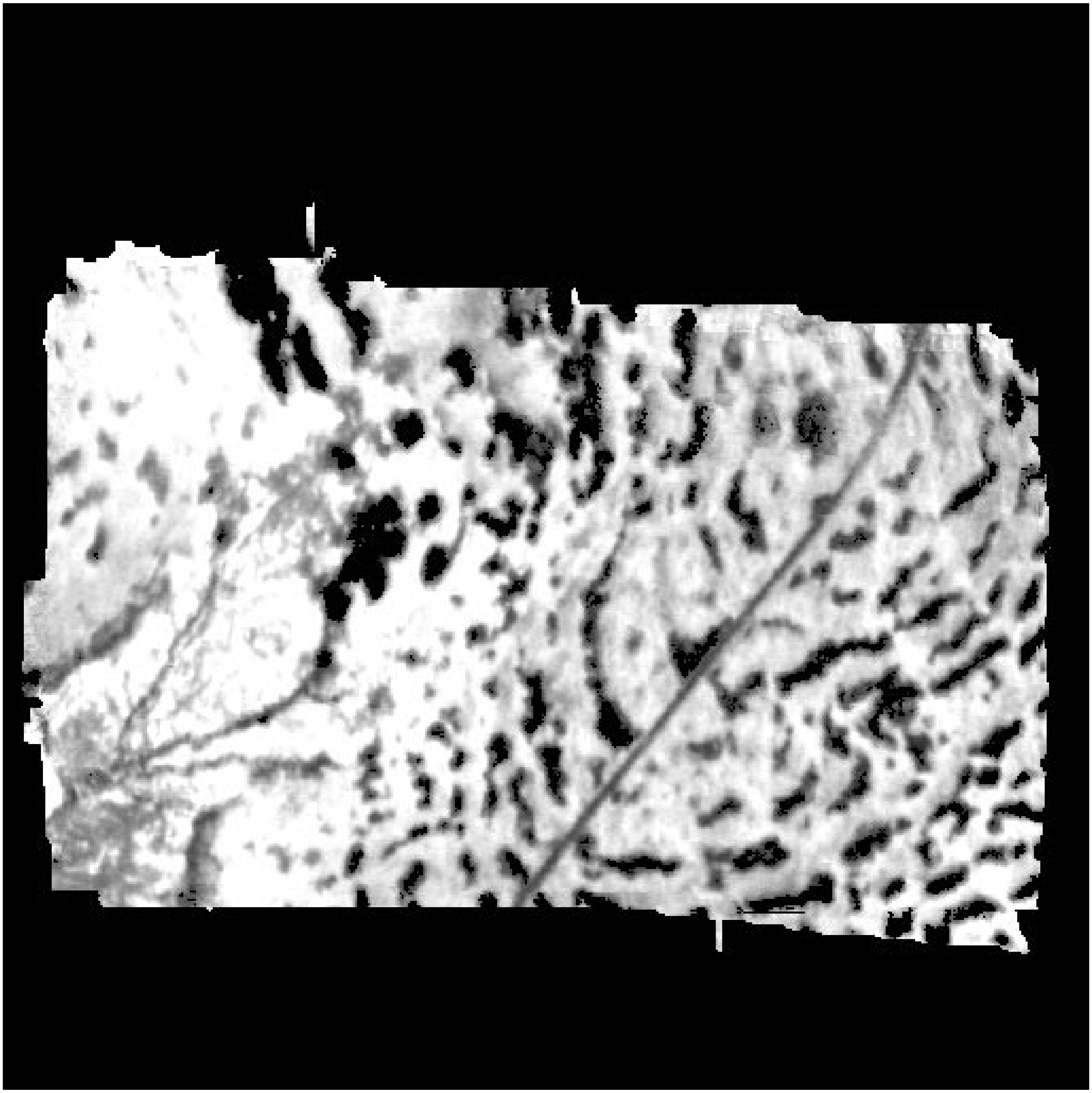

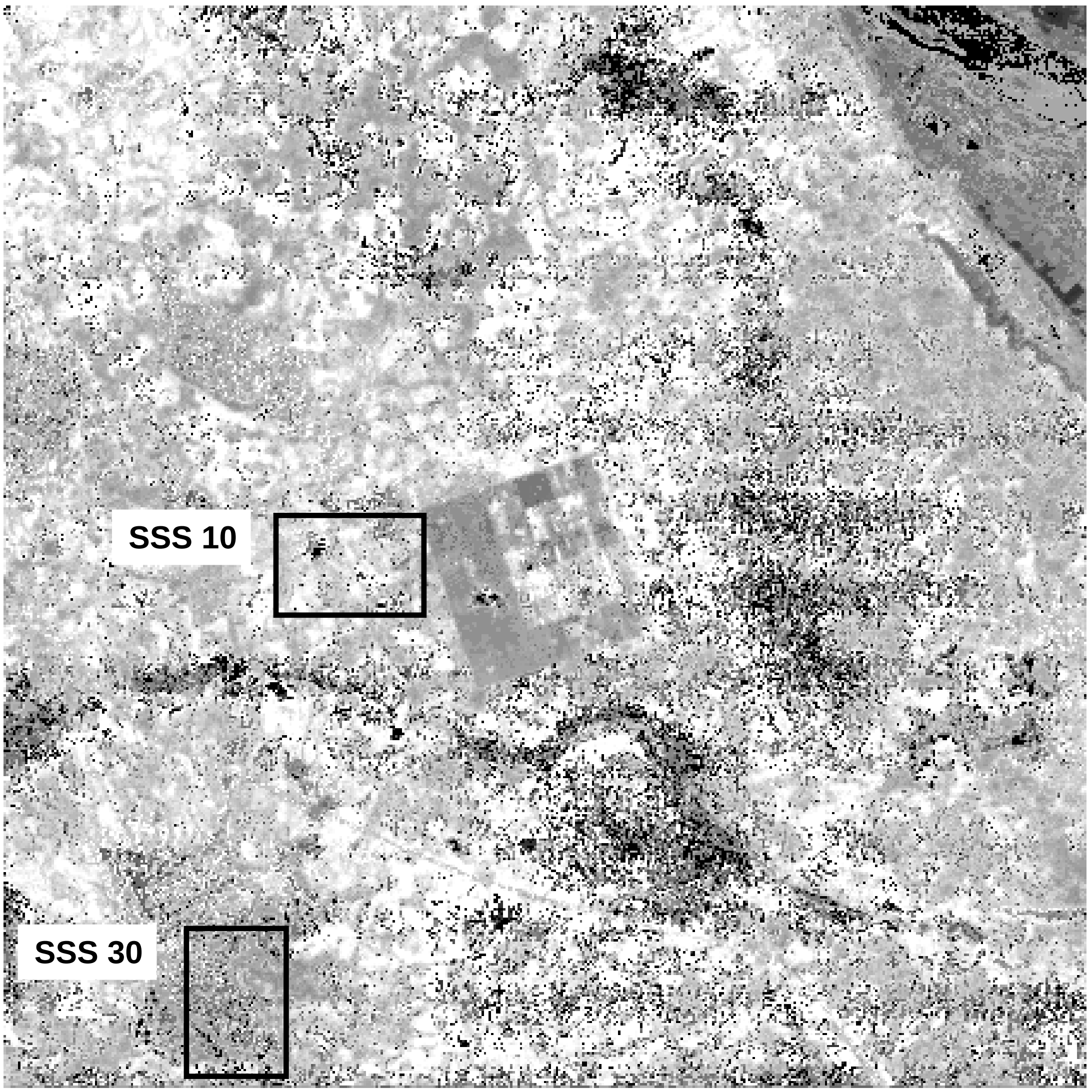
SSS 10
SSS 30